*Polar Record 43 (227): 290–304 (2007). Printed in the United Kingdom. doi:10.1017/S0032247407006420*

# Derivation and assessment of vegetation maps for reindeer pasture analysis in Arctic European Russia

**W.G. Rees and F.S. Danks**
Scott Polar Research Institute, University of Cambridge, Lensfield Road, Cambridge CB2 1ER

*Received March 2007*

ABSTRACT. Throughout northern Eurasia, the presence of reindeer is a complicating factor in the consideration of interactions between vegetation and climate. The ability to interpret future changes in these interactions will depend on access to maps of sufficient detail to represent aspects of vegetation distribution relevant to reindeer grazing, amongst which we particularly identify lichens and shrubs. Such maps, if they are to have circumpolar coverage, can only feasibly be produced on a routine basis using satellite imagery having wide swaths but comparatively coarse resolution. This paper presents qualitative and quantitative comparisons between three such maps, and two more detailed vegetation maps compiled from fieldwork and from recent field-trained satellite image analysis, all for a study area in the Nenets Autonomous Okrug, Russia. It is shown that, despite its high degree of generalisation, the Circumpolar Arctic Vegetation Map provides the best representation of the vegetation in the study area amongst the three circumpolar land-cover maps that were examined, but that none of the three is entirely satisfactory. While the adequate representation of shrubs and lichens currently continues to depend on the analysis of field data or high-resolution satellite imagery which is unsuitable for circumpolar mapping, it is suggested that the prospects for satellite-based circumpolar vegetation mapping capable of including these components is promising.

**Contents**



## Introduction

The vegetation of the tundra regions north of the Arctic treeline can be expected to be a particularly sensitive indicator of global change, especially climate change, through its proximity to the limits of survival and the polar amplification of global warming (Cornelissen and others 2001; Skre and others 2002; van Herk and others 2002; van de Linden and others 2003; Stow and others 2004). In turn, the vegetation systems provide feedbacks to the global climate system (Betts 2000; Harding and others 2002), especially through modifications to the carbon and water cycles and through albedo feedback. Modelling and monitoring of vegetation distribution and of vegetation-climate interactions in the north are thus essential activities, but it is also important to take into account non-climatic perturbations to these interactions. These include regionally-generated and long range industrial pollutants (Rees and Rigina 2003), infrastructure and resource development, silviculture and agriculture.

In northern Eurasia, agriculture in the form of reindeer husbandry represents a significant form of land use. Reindeer pasture covers much of the European north, from the Arctic coast southwards to, and beyond, the treeline. Reindeer herding is a major component of the traditional livelihood of the indigenous peoples of the north, and has sustained them for many generations. At present there are perhaps one million reindeer (*Rangifer tarandus*) in the European north (Rees and others 2003), on an area of about 750,000 km$^2$ set aside for pasture (Fig. 1). About one fifth of these reindeer, and one third of the grazing area, are within European Russia (all data have been compiled from published sources as part of the authors' unpublished research). Such large numbers of reindeer have a profound influence on the ecology of the region, affecting the distribution and dynamics of vegetation (Käyhkö and Pellikka 1994; Kumpula and others 2000; Théau and others 2001; Rees and Rigina 2003; Théau and Duguay 2004; Tømmervik and others 2004). On the other hand, changes in the distribution of vegetation arising from climate change or other causes may have influences on reindeer grazing, pasture use and population trends (Klein 1999). Significant changes in tundra vegetation have already been reported (Hinzman and others 2005), notably an increase in the extent, density and height of shrubs (Silapaswan and others 2001; Sturm and others 2001; Hope and others 2003), decrease in the abundance of lichens (Cornelissen and others 2001), and the transformation of tundra areas formerly dominated by dwarf shrubs and lichens into largely graminoid tundras (Rees and others 2003). Ecosystem-based modelling implies that the area of tundra should shrink in response to climate change, as the boreal forest advances northwards (Skre and others 2002; ACIA 2004). The presence of reindeer is implicated in some of these trends; all of them are important for the ways in which reindeer husbandry is practised.

The ability to detect and assess changes in the distribution of arctic vegetation in future clearly depends on the availability of suitable baseline maps. Perhaps

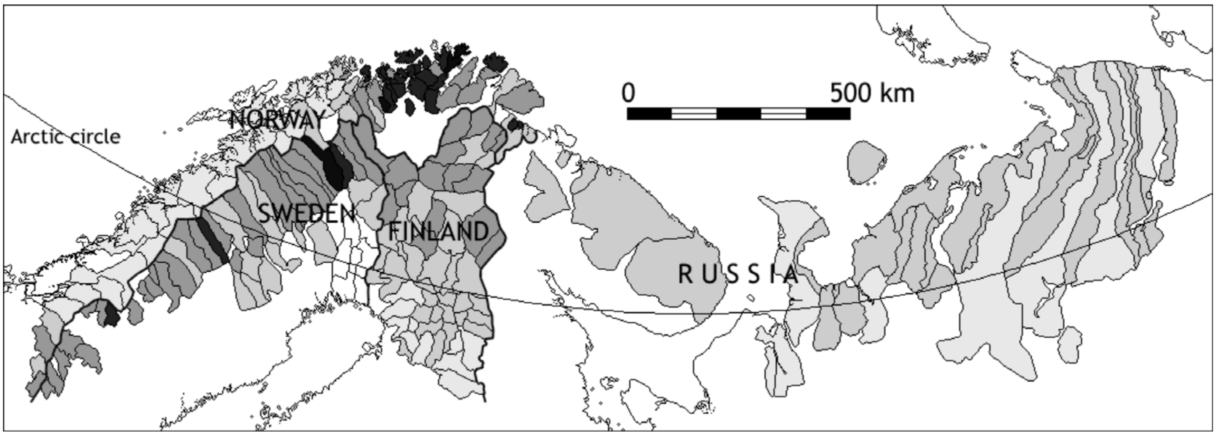


Fig. 1. Approximate distribution and grazing density of reindeer in Europe, compiled by the authors from official statistics current between 1997 and 2003. Darker greys correspond to higher densities. The data are aggregated at the 'lowest local administrative level', that is sovkhoz, kolkhoz, share company etc. in Russia, paliskunta in Finland, sameby in Sweden and distrikt in Norway. Data for winter pasture areas in Norway are not shown.

not surprisingly in view of its general remoteness, the vegetation of the circumpolar region is not presently known in great detail (Walker and others 1995; Rees and others 2002; CAVM Team 2003). Detailed vegetation or ecological maps exist for some areas, although these are usually rather limited spatially and very far from being able to give a circumpolar perspective. They are also inherently rather slow to update. It is thus likely that baseline vegetation maps will be reliant on coarser-resolution and more generalised maps based at least to some extent on satellite imagery.

The aim of this paper is to assess the suitability of different types of vegetation map for describing and analysing the interactions between reindeer grazing and vegetation. The maps vary in spatial resolution from tens of metres to several kilometres, and also vary considerably in the extent to which fieldwork is used in their compilation. Specifically, the extent to which different maps contain the same information is quantified. A study area in Russia is chosen on the basis that this is generally the least well mapped part of the Arctic, so that it is particularly important to assess the suitability of different approaches to land-cover mapping in that country.

## Scaling

An important concept inherent in this work, and indeed in many sciences concerned with human activity and physical processes on the Earth's surface, is that of scaling (Quattrochi and Goodchild 1997; Marceau 1999). Many environmental processes, such as the impact of climate change on an ecosystem, require an understanding of how processes operate at different scales and how they are linked across scales. Scale is increasingly recognised as a central concept in describing the hierarchical organisation of the world, and the establishment of a science of scale has been proposed (Marceau and Hay 1999). One approach to the difficulty of accounting and allowing for the effects of scale and aggregation in statistical data and mathematical modelling of complex ecological systems is through the concept of the 'scaling ladder' (Wu 1999). This combines aspects of hierarchy theory, which treats ecological systems as approximately decomposable because of their loose coupling, and patch dynamics, which deals explicitly with spatial heterogeneity. Wu's scaling ladder is a hierarchical strategy that consists of three broad stages: (1) identification of appropriate patch hierarchies; (2) observing and modelling patterns and processes at focal levels; (3) extrapolation across the domains of scale using a hierarchy of models. In particular, such an approach is highly relevant to the problem of validating land-cover maps, especially those derived from coarse-resolution satellite data, using stratified random sampling of field data (Lunetta and Lyon 2004). We adopt a simpler approach to the task of accounting for some of the scale-dependent differences between maps, and then discuss the relationship between or approach and the scaling ladder.

## Study site and characteristics

We selected the territory of the Vyucheiskiy Kolkhoz (collective farm) as our study area. This territory is located within the Nenets Autonomous Okrug (NAO) in northeastern European Russia (Fig. 2). The area of this territory is approximately 10,000 $km^2$, on which typically 8,000–12,000 semi-domesticated reindeer are grazed, representing roughly 1% of both the entire European population of reindeer and area of grazing. The kolkhoz is administered from the village of Nelmin Nos. The territory is situated in the tundra zone north of the treeline, north of the delta of the river Pechora. It is generally low-lying, mostly below 100 m. The lowest-lying ground is found in the Pechora Delta, the delta of the river Neruta, and the large peninsula in the northeastern part of the region. The annual average temperature at Nar'yan-Mar, the administrative centre of the NAO

https://doi.org/10.1017/S0032247407006420 Published online by Cambridge University Press

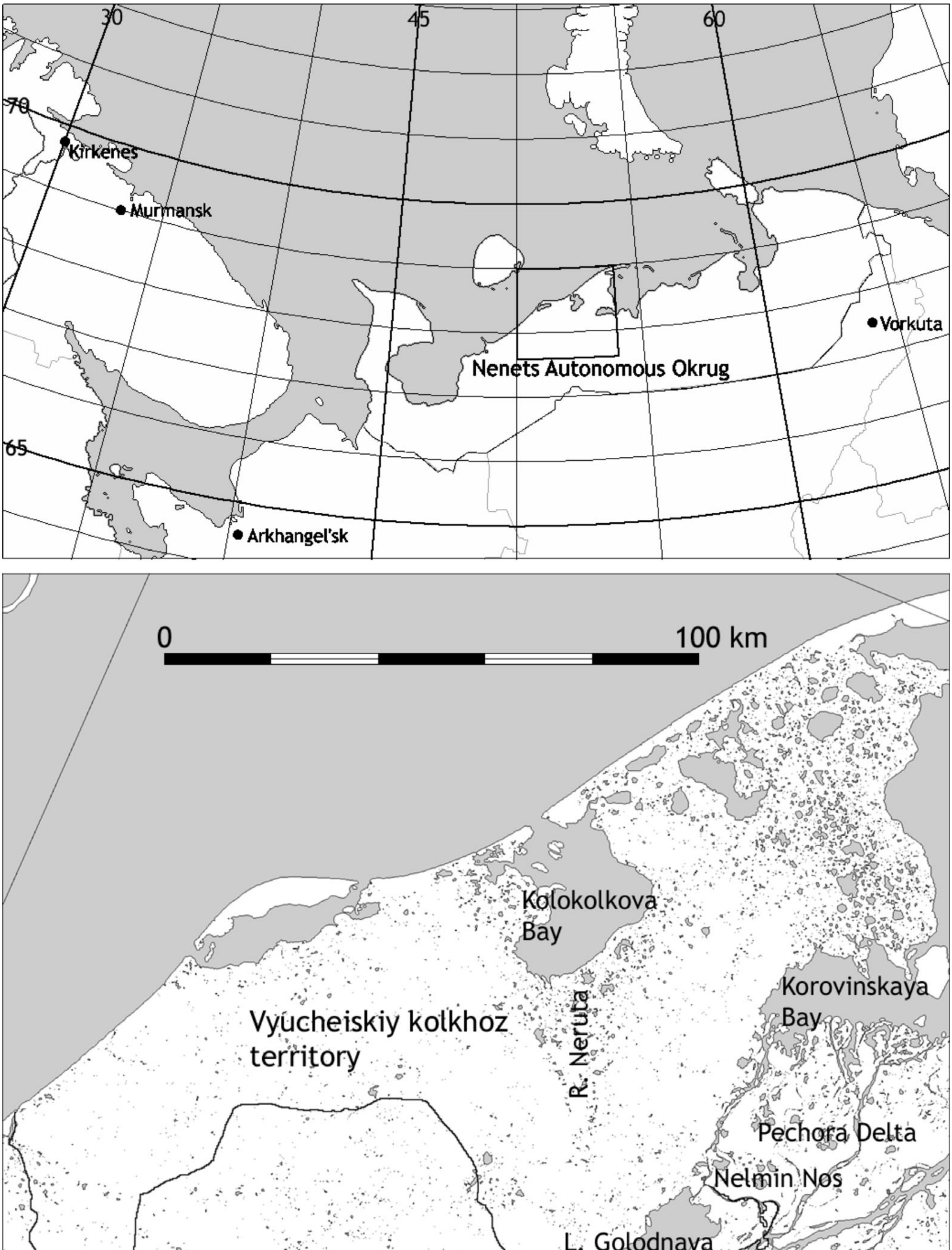


Fig. 2. Location of the study area. The oblique straight lines show the coverage of the Landsat image discussed later.

https://doi.org/10.1017/S0032247407006420 Published online by Cambridge University Press

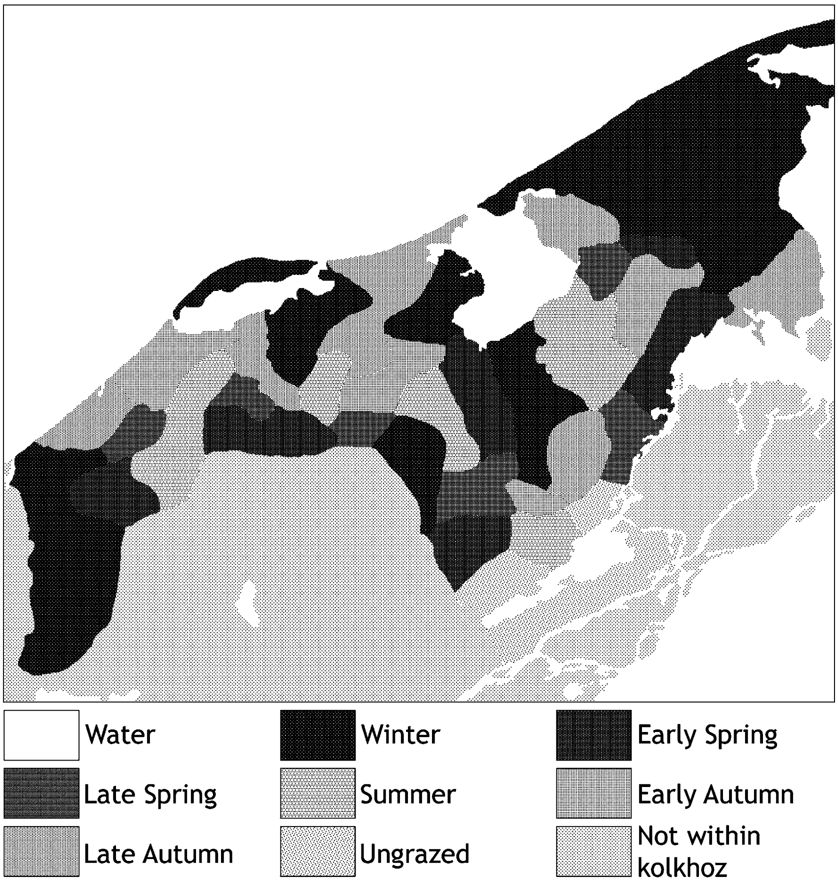


Fig. 3. Official grazing map for the Vyucheiskiy kolkhoz showing the seasonality of pasture.

which lies on the Pechora River and within the study region, is −3.6°C and the annual average precipitation is 430 mm.

Reindeer in the Vyucheiskiy Kolkhoz, like most domesticated reindeer in Russia, are managed by 'close herding', which involves full-time husbanding of the herd by a team (normally a family group) of herdsmen as they guide the animals along their annual migration route over unfenced terrain. The migration of a herd, which can often cover hundreds of kilometres annually (although the distances are rather less in this Kolkhoz), is supposedly governed by official regulations using highly detailed maps specifying the number of reindeer grazing days provided by each parcel of land. The extent to which these regulations and maps are followed has declined in the years since they were drawn up, probably in the 1970s, and especially since the dissolution of the Soviet Union. Nevertheless, the basic principle of seasonality of pasture has largely survived. According to this principle, grazing typically follows a 6-season pattern (winter, early and late spring, summer, early and late autumn) intended to reflect, *inter alia*, seasonal variations in diet. Lichens form a particularly important component of the reindeer diet during the winter, in this area as in many others; conversely, herdsmen attempt to keep reindeer away from lichen stands during the summer when they are dry and susceptible to mechanical damage by trampling. The pasture seasonality is shown in Fig. 3. This figure was derived from the official grazing map of the Kolkhoz, a paper map with no graticule or projection data. Unfortunately we do not possess citation data for it. The paper map was digitised and georeferenced to large-scale (1:200,000) maps of the region, with an estimated error of around 2 km.

## Land-cover maps of the study area

The most generalised maps of the study area are usually extracted from global or circumarctic maps having a spatial resolution of the order of 1 km, often derived at least in part from global-coverage satellite imagery. An important example of such a map (the term will be used to include the more general concept of land-cover classification) is the database of global land cover characteristics generated by the United States Geological Survey Earth Resources Observation System (USGS EROS) Data Center, the University of Nebraska at Lincoln (UNL), and the Joint Research Centre (JRC) of the European Commission. This database, which covers the entire global land surface at a resolution of about 1 km, is derived from AVHRR 10-day composites from April

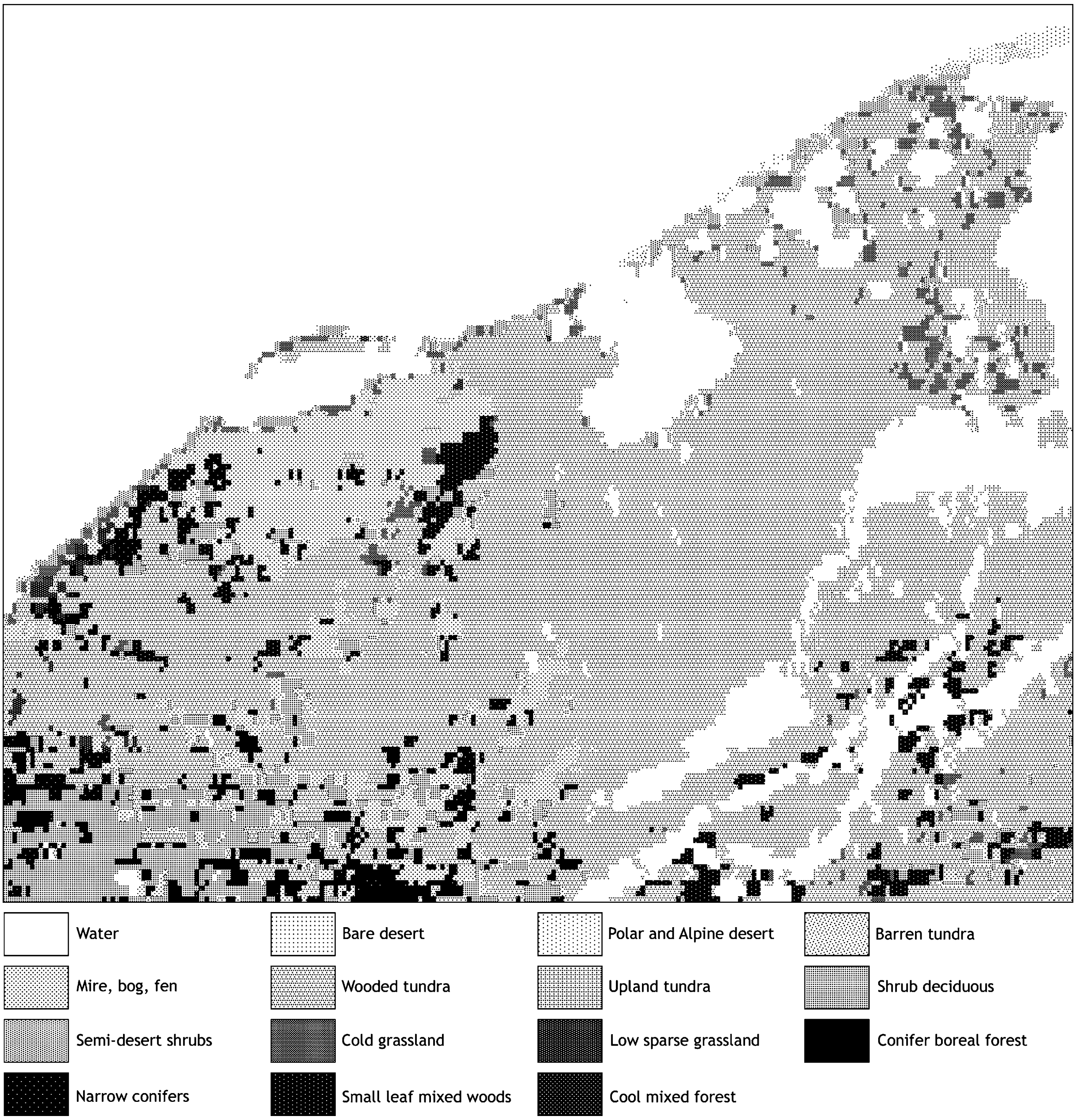


Fig. 4. Olson classification of the study area. Water areas have been masked out.

1992 to March 1993 (Eidenshink and others 1994) and other ancillary data including Digital Elevation Models (Brown and others 1993). Specifically, we use the version of the database that classifies regions according to Olson's (Olson 1994a, 1994b) classification of global ecosystems. This represents the global land surface by approximately 90 different land-cover types, although naturally many of these do not occur in the Arctic (Fig. 4). For simplicity, we refer to this database, which was downloaded from http://edcsns17.cr.usgs.gov/glcc (last access 26 July 2005), as the Olson classification.

Similar to the Olson classification is the Global Land Cover Classification for the year 2000 (GLC2000), produced by the JRC (European Commission 2003) using data from the instrument VEGETATION carried on the SPOT-4 and SPOT-5 satellites. This map is illustrated in Fig. 5.

The third of the global-coverage maps that was used to derive a land-cover classification of the study area was the Circumpolar Arctic Vegetation Map (CAVM). The CAVM (Walker and others 2002; CAVM Team 2003) describes the circumarctic vegetation north of the treeline in terms of 15 generalised physiognomic units based on the growth forms of plants. It was produced at a scale of 1:7.5 million, giving it a spatial resolution of the order of 5 km, and was based on AVHRR imagery and local field data from some areas. The CAVM coverage of the study area is shown in Fig. 6.

https://doi.org/10.1017/S0032247407006420 Published online by Cambridge University Press

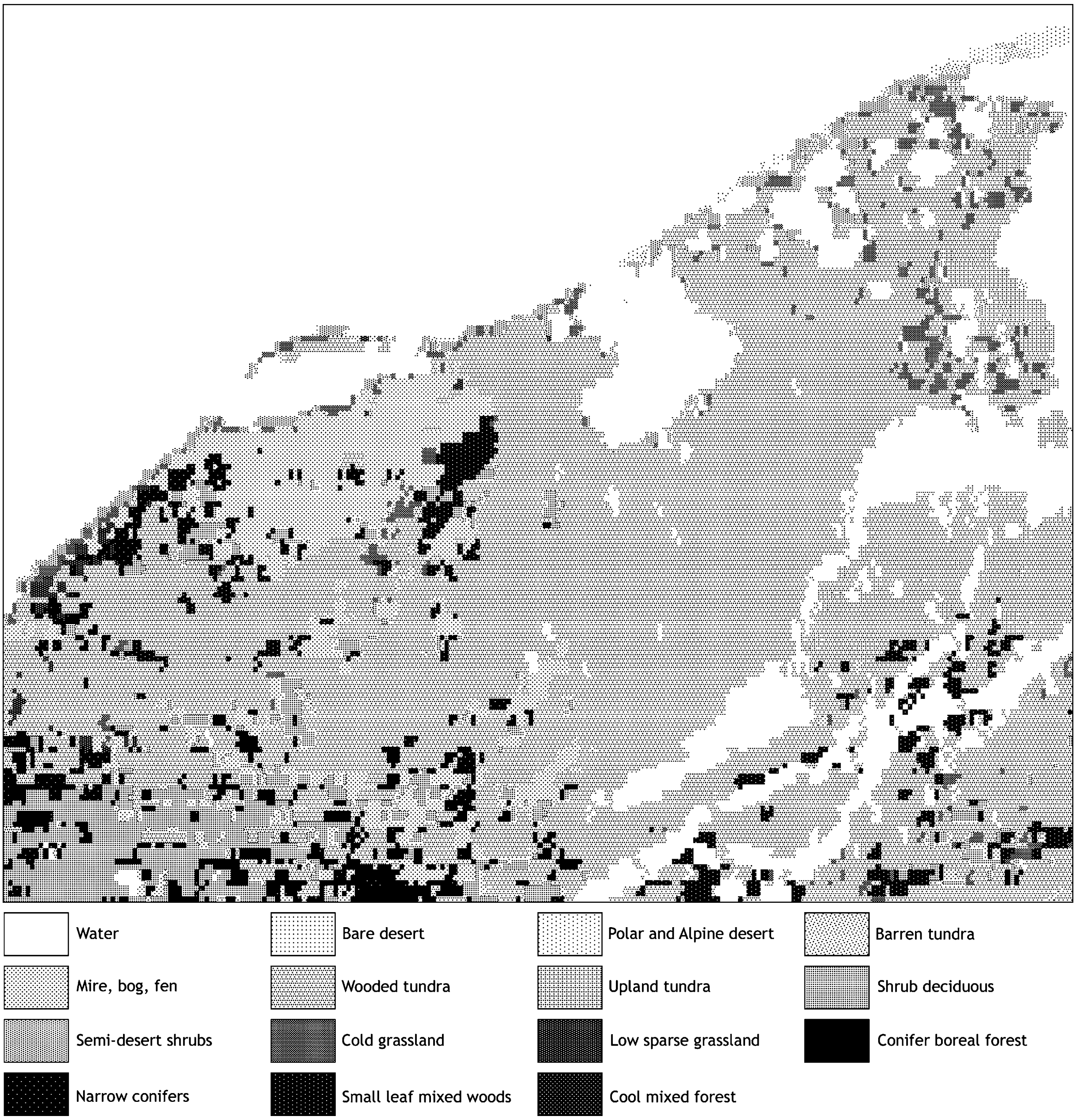


Fig. 5. JRC GLC2000 classification of the study area.

One larger-scale vegetation map of the study area was acquired. This was part of a more extensive vegetation map compiled in the 1970s (Isachenko and others 1974), which we refer to as the Russian vegetation map (RVM). It was obtained as a scan of a paper map with a latitude-longitude graticule that permitted reprojection. The pixels of the scanned image corresponded to a size of around 200 m, and the absolute locational accuracy of the map was estimated to be around 1 km. The map was georeferenced and reprojected into a simple geographical (Plate Carrée) coordinate system with a grid spacing of 0.00400 degree in longitude and 0.00167 degree in latitude, subsetted to a range of 50 to 54 degrees in longitude, 67.6 to 69 degrees in latitude (image size 1000 × 840 pixels). (This projection and resolution was used for all maps.) The RVM is shown in Fig. 7.

## Landsat image classification

To provide a detailed and up-to-date reference against which these land-cover maps could be compared, a new map was compiled. This was done on the basis of a Landsat-7 ETM+ image, path 175, row 012, acquired on 29 June 2000. This image was acquired under cloud-free conditions and appeared to be of excellent quality apart from a few rows of corrupt data in band 4. Its coverage was close to ideal for the study area, as indicated in Fig. 2. Training data for the image classification were acquired during two field seasons, from 5 July to 2 August 2003 and from 17 July to 14 August 2004 (a few points were also

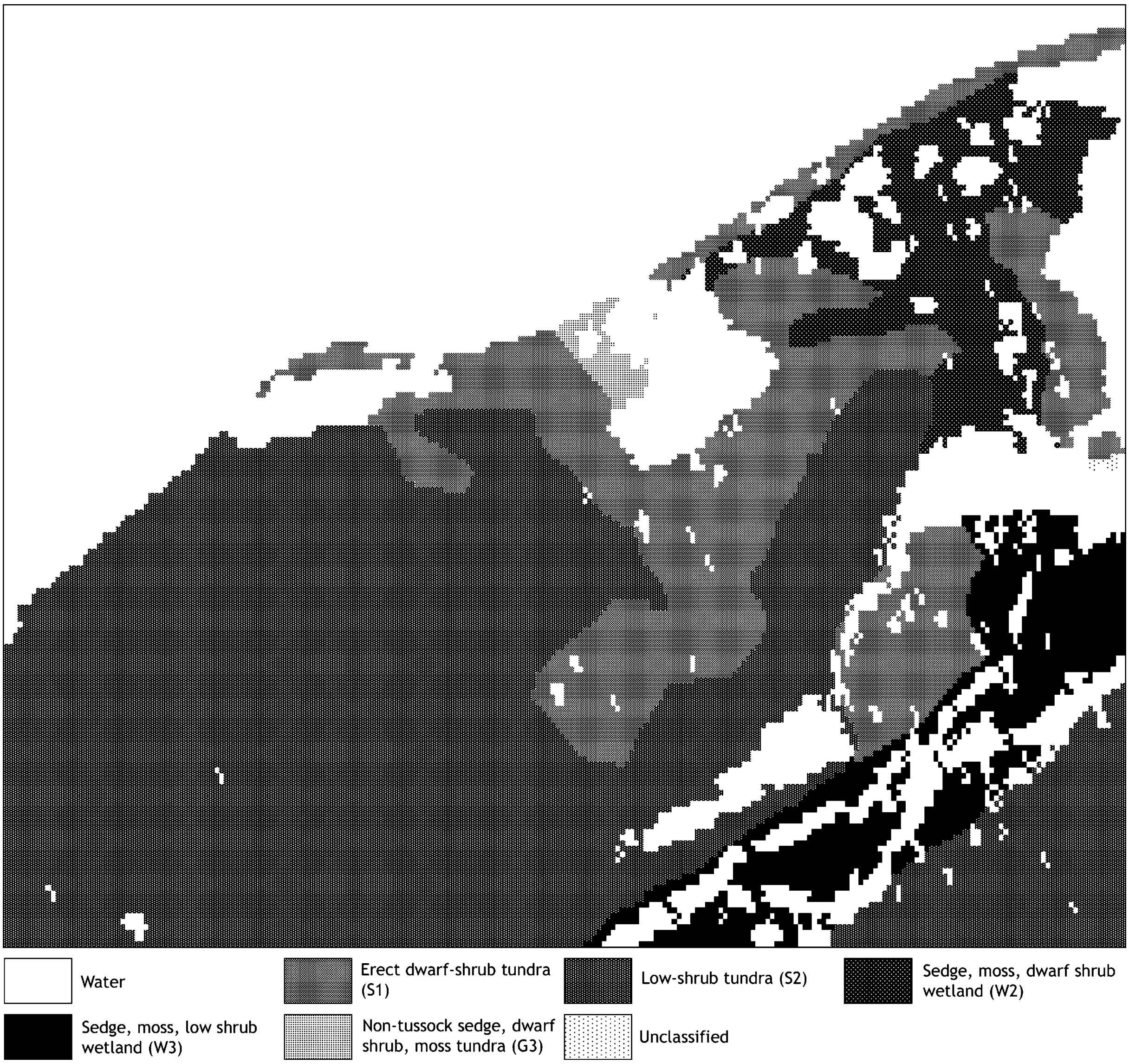


Fig. 6. Extract of CAVM for our study area. Water areas have been masked out.

collected during fieldwork in July 1999). During these periods of fieldwork we lived and migrated with a group of Nenets reindeer herders, making many excursions on foot for the purpose of data collection. Opportunities for data collection were also taken during the approximately 25 km journey from the village of Nel'min Nos to the herders' campsite by all-terrain vehicle, and during the 50 km boat journeys between Nar'yan Mar and Nel'min Nos. In total, data were collected from around 250 sites, with locations determined to an accuracy of around 10 m using handheld GPS, covering all seasonalities of pasture (Fig. 8). More field sites would of course have been preferable, but in practice the possibilities for data collection were somewhat limited by the unavailability of any form of mechanised transport on the tundra, the difficulty of moving by foot over the terrain, and the absolute necessity of not hindering the management of reindeer. A more extensive distribution of field sites would also have been preferable, but was not feasible for the same reasons. However, we are confident that the range of terrain and land cover types explored during the fieldwork in 2003 and 2004 was sufficiently representative of the entire kolkhoz territory, as a result of many hundreds of kilometres of helicopter overflight, extending over much of the territory, undertaken by the first author in 1999.

Each field site was chosen to have homogeneous land cover over an area represented by several pixels (preferably more than 9, although the extreme heterogeneity of the land cover in some places made this difficult to achieve) in the reflective, non-panchromatic bands of the Landsat image. Sites were selected on the basis of preliminary (pre-fieldwork) unsupervised classification of the image, and observations during fieldwork. Sites were identified by their GPS location, the date of visit, a unique site number and a general description of landscape at the pixel scale (30-300 m). Detailed species composition data were collected for all sites.

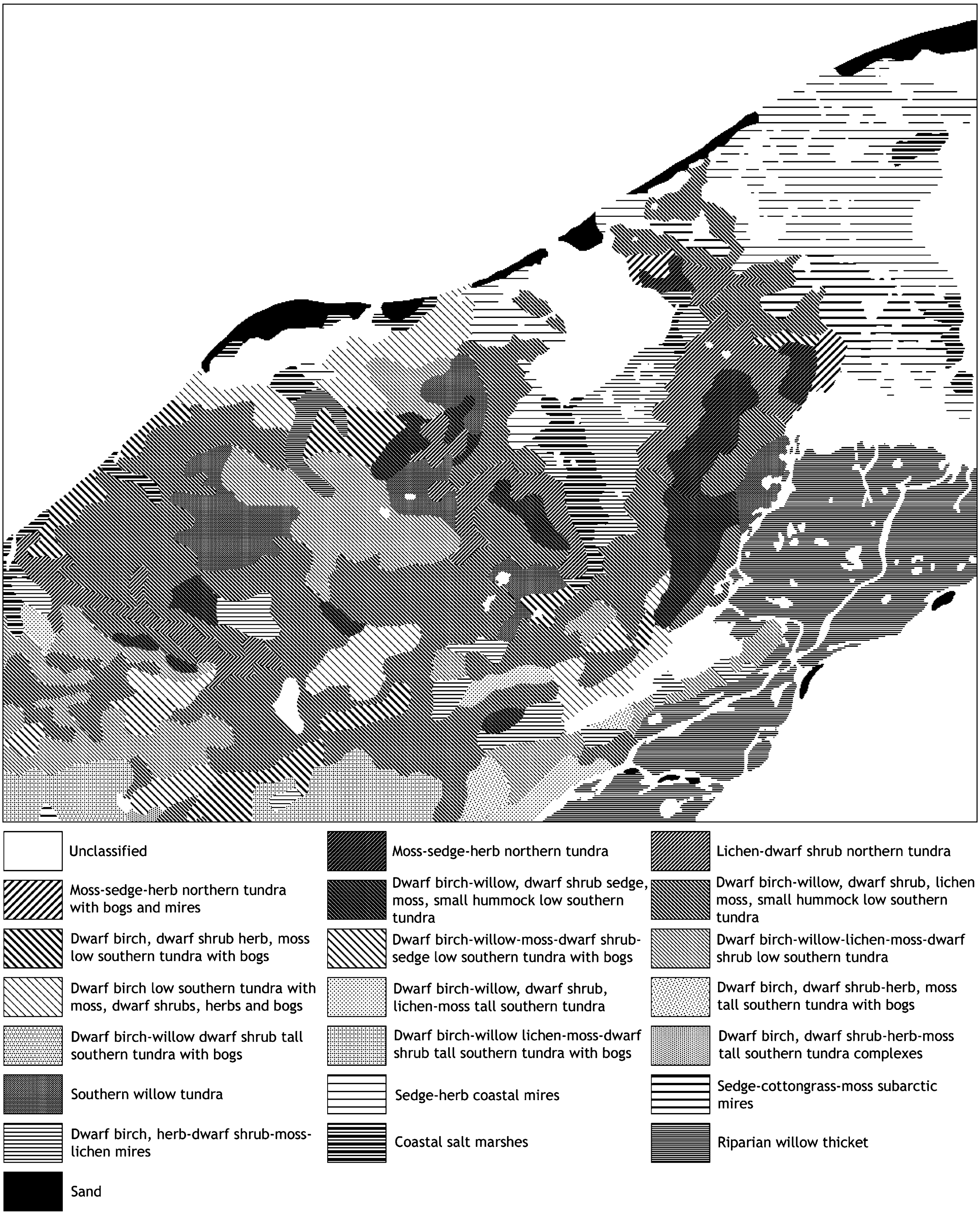


Fig. 7. Russian vegetation map (Isachenko and others 1974).

The image was first averaged to a pixel size of 120 m in all bands to reduce the total data volume, and to force a greater degree of homogeneity and generalisation on the classification, in recognition of the comparatively limited opportunities to collect training data. Even so, the resolution of the image was still substantially higher than that of any of the land-cover maps against which it was to be compared. Classification of the image proceeded as follows. First, training areas corresponding to deep, shallow and turbid water were defined directly from the image, using 1:200,000 scale topographic maps as corroboration where needed. A supervised classification was performed at this stage, to identify areas of water and mask them from subsequent processing. The second

https://doi.org/10.1017/S0032247407006420 Published online by Cambridge University Press

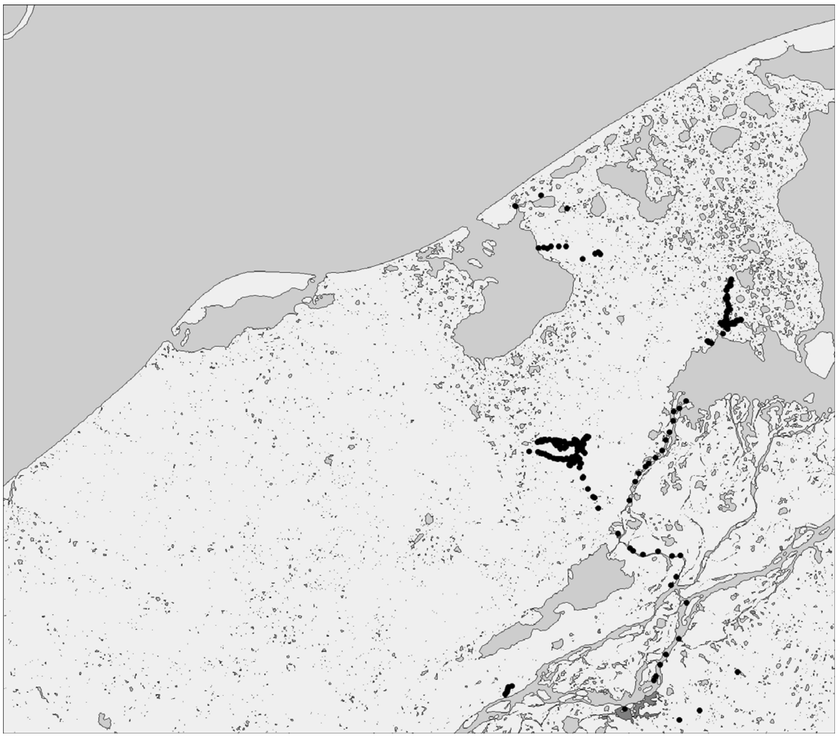

Fig. 8. Location of 250 field sites used to train the image classification.

step was to identify areas of shrub vegetation and, in the south of the area (and outside the reindeer pastures), trees. This was done by calculating the normalised difference vegetation index (NDVI) for the image, using calibration data obtained from the Landsat web site. Dark-pixel subtraction was used to correct for atmospheric effects. The NDVI image was assigned a threshold at a value of 0.60 (determined by comparing the field site characterisations with the NDVI values), higher values being assumed to correspond to shrubs and trees. Again, these areas were masked from subsequent processing. The third major land-cover type to be extracted was bare ground. This was done using the technique of spectral purity, since a preliminary analysis showed that bare ground as a land-cover category could be unambiguously recognised in this way. As before, this category was masked from further processing. The remaining, unmasked areas were classified by first performing an unsupervised classification initialised to 30 clusters. This converged to 13 clusters, which were assigned to the following four very generalised land-cover classes on the basis of the field training data and (where necessary) the topographic maps: dry heath, moist heath, wetlands (fens, bogs and mires), water-vegetation mixtures or submerged vegetation. No attempt was made to distinguish between lichen-rich and lichen-poor areas because of the usually small size of the typical lichen stands noted during our fieldwork. Thus, the final classification consisted of six land-cover categories plus water, as shown in Fig. 9.

A qualitative assessment of the effect of first reducing the resolution of the Landsat ETM+ image and then classifying it was made by, in effect, reversing the process. The full-resolution image was classified using a hybrid supervised-unsupervised approach, initially into 40 image classes. These classes were merged to the same level of generalisation, similarly to the hyper-clustering approach (Myers and others 1999; Cihlar and others 2000), to confirm qualitatively that no significant differences in classification were found.

Error assessment of the satellite-derived land-cover classification is not straightforward, since the number of training data points did not really allow the recommended procedure to be adopted under which half of the data are used for training and the other half for error assessment. This is not an uncommon situation in satellite-based mapping of remote arctic regions, especially in Russia. Nevertheless, a standard error matrix was computed and used to calculate the producer's and consumer's (user's) accuracies, and the kappa accuracy (Cohen 1960; Monserud and Leemans 1992), excluding the water and water/vegetation categories (Table 1). Apart from the wetland category, which showed some confusion with moist heath and had a user's accuracy of only 0.52, all other categories had user's accuracies of at least 0.80. Producer's accuracies were above 0.71 for all classes except bare ground (confused with wetland and dry heath), with an accuracy of 0.53. The Cohen kappa value for the error matrix was 0.696. These figures are perfectly reasonable, apart from the two low individual accuracies and their effect on the value of kappa. However, the test is not truly independent of the process by which the classification was performed and hence may overestimate the accuracy. On the other hand, confidence

https://doi.org/10.1017/S0032247407006420 Published online by Cambridge University Press

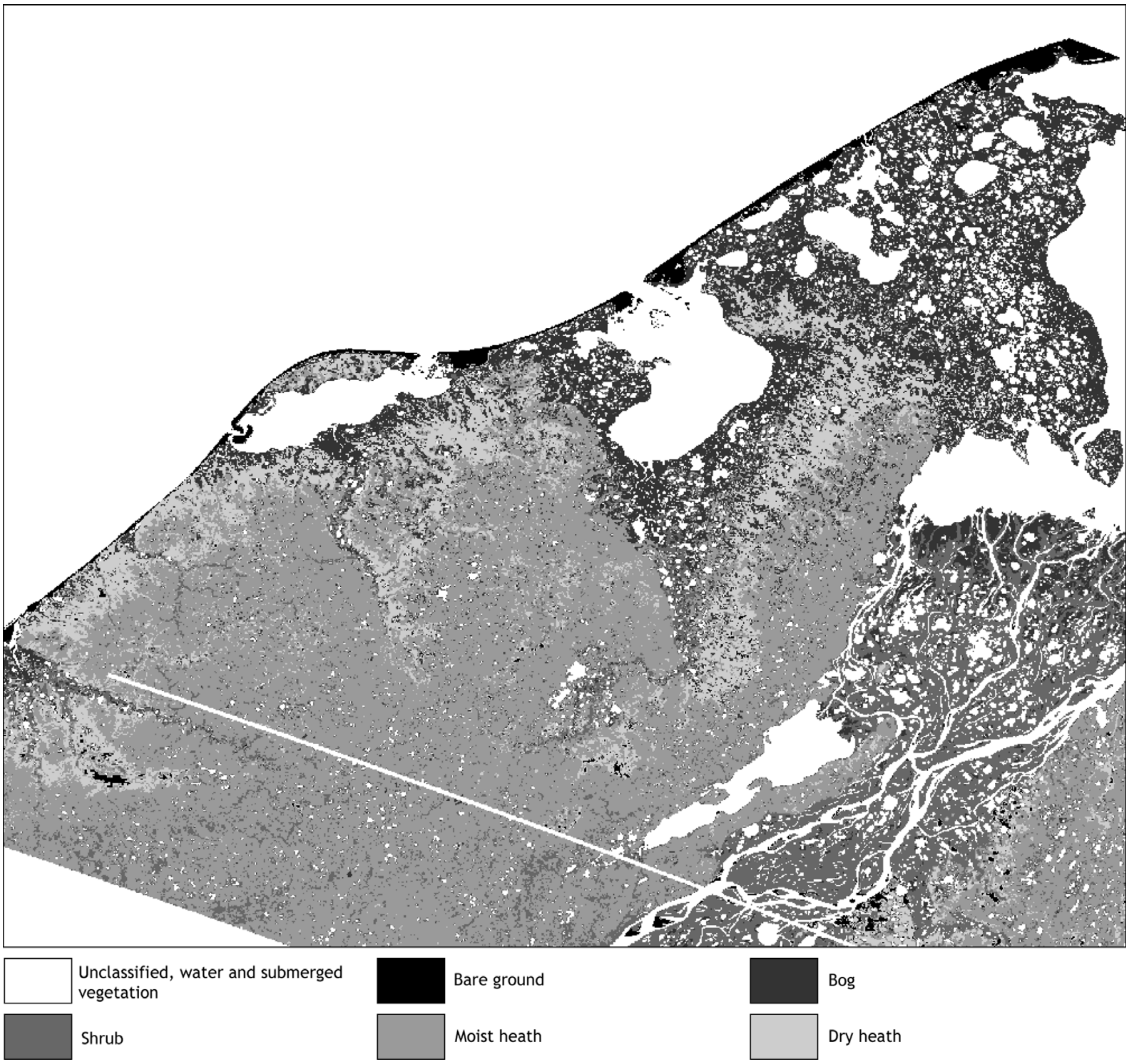


Fig. 9. Land cover map derived from classification of Landsat-7 ETM+ image.

is lent to the classification by two observations: (1) repeated attempts at classification, both supervised and unsupervised, and using both standard maximum-likelihood classifiers and spectral-spatial classifiers, show a high degree of stability in the spatial distribution of the general categories; (2) the distribution of land-cover types is not unexpected. The densest shrubs occur in the river deltas; bare ground occurs (as sand) predominantly along the sea shore but also in smaller spots on higher ground; wetlands occur on flat ground not drained by the major rivers; and dry heath occurs mainly on the west- or northwest-facing slopes, suggesting a meteorological origin of the distinction between moist and dry heaths.

Table 1. Error matrix for the Landsat ETM+ classification. Values are given in square metres.

| | | Training class | | | | |
|---|---|---|---|---|---|---|
| | | Bare | Dry heath | Moist heath | Wetland | Shrub |
| Image classification | Bare | 115200 | 0 | 0 | 0 | 0 |
| | Dry heath | 43200 | 720000 | 86400 | 0 | 0 |
| | Moist heath | 0 | 129600 | 907200 | 43200 | 43200 |
| | Wetland | 57600 | 57600 | 259200 | 475200 | 57600 |
| | Shrub | 0 | 14400 | 14400 | 28800 | 518400 |

https://doi.org/10.1017/S0032247407006420 Published online by Cambridge University Press

Table 2. Basic properties of the six maps considered in this work.

| Map | Input data | Compilation | Resolution (m) | No of categories in kolkhoz |
|---|---|---|---|---|
| Olson | AVHRR, DEM | 1994 | 925 × 350 | 16 |
| JRC GLC2000 | VEGETATION | 2000 | 1000 × 380 | 16 |
| CAVM | AVHRR, DEM, ancillary data | 2003 | ~ 5000 | 5 |
| RVM | Fieldwork | 1974 | ~ 500 | 17 |
| Pasture map | ? | ? | ~ 2000 | 6 |
| Landsat | ETM+ image, fieldwork | 1999-2003 | 120 | 7 |

## Comparing the land-cover maps

The properties of the six available land-cover maps of the study area (Olson, JRC, CAVM, RVM, Landsat classification and the pasture map of Fig. 3) are summarised in table 2. The second column shows the principal sources of data for each map, the fourth the resolution at latitude 67.6 °N, and the fifth the number of map categories present within the area of the Vyucheiskiy Kolkhoz.

Qualitative inspection of the maps reveals some strengths and weaknesses. The Olson classification (Fig. 4) contains a relatively large number of land-cover types, dominated by the 'wooded tundra' category. This map category is shown as occurring virtually everywhere between the Pechora delta and the river Neruta, and very largely throughout the peninsula north of Korovinskaya Bay (the secondary land-cover type shown here is 'cold grassland'). Both of these regions are known from fieldwork to contain a diversity of land-cover types, dominated by neither 'wooded tundra' nor 'cold grassland'. The Olson classification also significantly fails to identify the wetland areas of the Neruta and the Pechora delta. The JRC GLC2000 classification (Fig. 5) contains an equally large number of land-cover types, but their spatial distribution appears qualitatively more similar to that of the Landsat classification (Fig. 9), and is not overwhelmingly dominated by a single category. The riparian vegetation around the Neruta and Pechora rivers is represented, although the classification appears to under-represent shrubs. It also classifies a large proportion of the peninsula north of Korovisnkaya Bay as water, rather than as bogs and marshes. The CAVM (Fig. 6) is much less detailed than either the Olson or the GLC2000 classifications. However, the shapes of the land-cover units correspond well with the known distribution of vegetation, with the exception that it fails to identify the wetlands around the Neruta river. The vegetation map of Isachenko and others (1974) appears very plausible in the light of our simpler Landsat classification, and it is noteworthy that it is the only classification the key of which makes explicit mention of lichens.

In order to make a more definite comparison between these maps, a quantitative measure of map similarity is required. This task is complicated by the fact that the maps do not employ the same categories of land cover, and in fact, as emphasised by table 2, do not even use the same numbers of categories. Rather than attempting subjectively to identify equivalent categories between maps, with the consequent necessity to group some categories together, a measure of map similarity (meaning the extent to which one map can be used to predict the other) is adopted that essentially ignores the names of the map categories. Such a measure can be derived from the techniques of nominal (or categorical) association in statistics. These techniques are generally based on the use of the contingency matrix describing the joint probability of a particular pixel receiving one classification in the first map and another in the second map. One of the simplest and best known of the measures of nominal association is Cramér's V statistic (Cramér 1999). We use the square of this value, which we denote by F and which can be defined as follows:

$$F = \frac{1}{N(\min(m,n)-1)} \sum_{i=1}^{m} \sum_{j=1}^{n} \frac{(c_{ij} - c_{ij}^{*})^2}{c_{ij}^{*}} \qquad [1]$$

In this expression, an element of the contingency matrix, is the number of pixels (or area) that are assigned to category $i$ in map 1 and to category $j$ in map 2, where the total number of categories in map 1 is $m$ and in map 2 is $n$. $N$ is the total number of pixels in (or area of) the entire map and

$$c_{ij}^{*} = \frac{1}{N} \sum_{k=1}^{m} c_{kj} \sum_{k=1}^{n} c_{ik} \qquad [2]$$

The value of $F$ is normalised, such that it ranges between zero (indicating a purely random relationship between the two maps) and one (complete spatial coincidence between the maps as far as is allowed by the different numbers of categories). It is symmetric, in the sense that it is unchanged if the identities of maps 1 and 2 are transposed even if they have different numbers of categories. It differs in this sense from some other measures of nominal association such as the uncertainty coefficient (Theil 1972; Finn 1993).

All the maps were reprojected to the same projection: a Plate Carrée projection with 600 pixels per degree of latitude and 250 pixels per degree of longitude, and an extent between 67.6° and 69° N, 50° and 54° E. This gave an image size of 1000 × 840 pixels and a pixel size of around 170 × 185 m at the southern boundary of the maps, meaning that most of the original maps were interpolated while the Landsat classification was

https://doi.org/10.1017/S0032247407006420 Published online by Cambridge University Press

Table 3 Normalised similarity index *F* between pairs of maps.

| *F* | Olson | JRC | CAVM | RVM | Pasture |
|---|---|---|---|---|---|
| JRC | 0.142 | | | | |
| CAVM | 0.265 | 0.310 | | | |
| RVM | 0.277 | 0.195 | 0.465 | | |
| Pasture | 0.176 | 0.202 | 0.246 | 0.315 | |
| Landsat | 0.309 | 0.251 | 0.322 | 0.366 | 0.182 |

subsampled. In all cases, nearest-neighbour resampling was used.

Once the maps had been brought to a common projection, contingency matrices were calculated between all 15 pairs of maps, and these were used to evaluate the similarity statistic *F* from equation (1). The results are shown in table 3.

As a way of visualising the matrix of similarities in table 3, we performed a multidimensional scaling (or principal coordinates) analysis (Gower 1966). This calculates the coordinates assigned to points representing each map in an abstract 6-dimensional (because there are 6 maps) space, such that the Euclidean distance between any pair of points is 1-*F* where *F* is the corresponding similarity for the pair of maps. The order of the dimensions is chosen such that the first dimension contains most of the variability, followed by the second dimension, and so on. In this case the first two dimensions contain more than half of the total variance, so a diagram representing them (Fig. 10) captures most of the information in table 3.

## Discussion

Table 3 and Fig. 10 show that, of the six maps that were analysed, the three that are most like another are the CAVM, the Russian Vegetation Map and the Landsat classification. These are diverse in terms of spatial resolution and number of categories, as demonstrated by table 2. However, what differentiates them from the other three maps is the extent to which *in situ* data have been used in their compilation, which is perhaps not an unreasonable connection. It is interesting to note that, despite its small number of categories (that is, high degree of generalisation), the CAVM is the best of the circumpolar/global maps at representing the distribution of vegetation within the study area. Again, this may not be particularly surprising in view of the fact that the CAVM is the only one of the circumpolar maps to have been 'optimised' for arctic vegetation (and it is conversely interesting to note how dissimilar the JRC classification is to most others). A third feature of table 3 and Fig. 10 is the dissimilarity of the pasture map (Fig. 3) to all other maps except the RVM. We do not know the process by which the pasture map was compiled, nor when, but it is not unreasonable to suppose that it could have been derived from the RVM.

Examination of the contingency matrices for each pair of maps amongst the three that are most similar (CAVM,

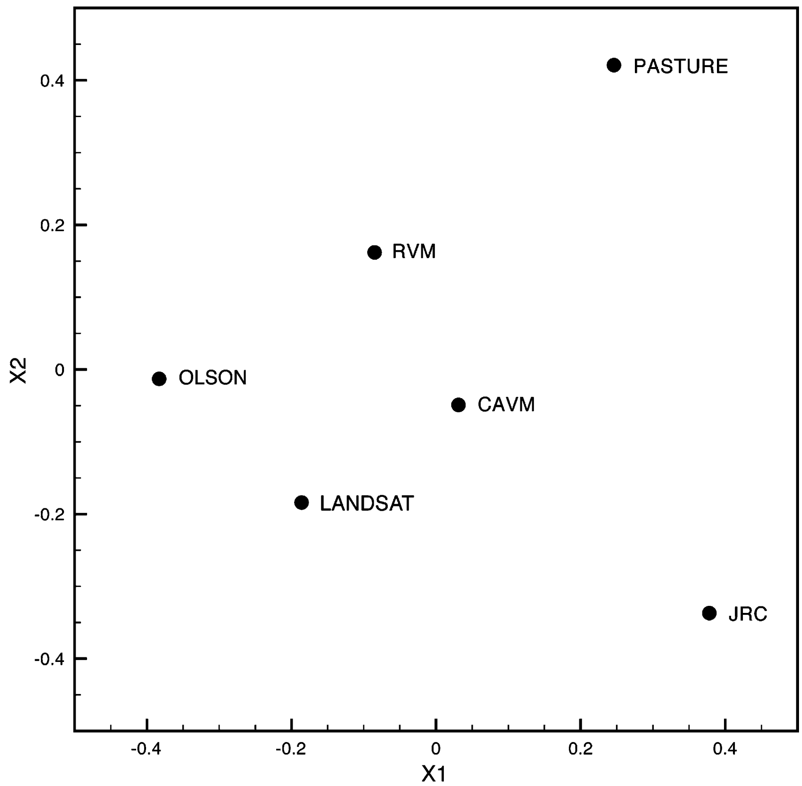


Fig. 10. Representation of the data in table 3 as the first two dimensions X1 and X2 in a multidimensional scaling analysis.

https://doi.org/10.1017/S0032247407006420 Published online by Cambridge University Press

RVM and the Landsat classification) reveals the extent to which particular categories in one map correspond to those in another map. We find that CAVM category S2 ('low shrub tundra') maps reasonably consistently onto the RVM category 'low dwarf shrub birch tundra with sparse shrub layer', and to the 'moist heath' category in the Landsat classification. Similarly, the CAVM category W2 ('sedge-moss-dwarf shrub tundra wetland), the RVM categories of 'mires' and the wetland category in the Landsat classification tend to coincide. On the other hand, dry heaths and shrubs are less consistently represented in the different maps, and this may perhaps be indicative of changes in both of these components of tundra vegetation over the last few decades, or it may simply reflect a greater difficulty in mapping them. Both of these categories are important, the former especially with regard to lichens. They are significant for reindeer husbandry, and their distribution is expected to change in response to changing climate. It is therefore important to consider the scope for improving their representation in circumpolar mapping.

The most promising sources of data for mapping the current distribution of arctic vegetation and identifying changes in future are the new coarse-resolution imaging instruments deployed from low-earth orbit satellites, such as MODIS and MERIS. MODIS (operational since 2000) is carried on board the Terra and Aqua satellites and acquires 36 spectral bands of data at a spatial resolution of 250, 500 or 1000 m, while MERIS (operational since 2002) is carried on board the Envisat satellite and acquires 15 spectral bands at a spatial resolution of 300 m. Both instruments provide for frequent viewing of any given location on the Earth's surface, from twice a week to several times per day. An extensive range of derived data products is already generated from both instruments. In particular, MODIS provides a land cover product MOD12Q1, although this is currently unsuitable for mapping arctic vegetation (for example within our study area it shows the majority vegetation type as shrubland, grass or crops). However, preliminary investigations by the authors (not described here) have suggested that, even at a spatial resolution of 1 km, MODIS data can give a clear distinction between tundra, shrubs and forest through the use of the normalised difference vegetation index (NDVI).

The ability to map the distribution of lichens is more open to question. Lichens generally have highly distinctive reflectance spectra (Käyhkö and Pellikka 1994; Théau and others 2001; Nordberg and Allard 2002; Rees and others 2004) and are phenologically stable compared to most background vegetation (Kershaw 1985; Nordberg and Allard 2002), and can readily be identified in high-resolution imagery. However, the spatial resolution of MODIS or MERIS data is rather coarse in comparison with the typical size of lichen patches. Successful attempts at mapping lichen distribution using remotely sensed imagery have been reported (Nordberg and Allard 2002; Sandström and others 2003; Tømmervik and others 2003; Stow and others 2004; Théau and Duguay 2004; Tømmervik and others 2004; Théau and others 2005), although none of these has made use of data having a spatial resolution coarser than that of Landsat TM or ETM+ (30 m). As far as the authors are aware, no research has been reported to produce reliable classification of lichens from coarse-resolution (250 m or coarser) satellite data. Nevertheless, the fact that lichen cover of only 20% can be discriminated from dry heath using Landsat imagery (Nordberg and Allard 2002) offers hope that the more spectrally diverse MODIS imagery may be able to achieve similar or better discrimination. Our preliminary investigations (not reported here) suggest cautious optimism that circumpolar lichen mapping is indeed feasible, and that it may therefore be possible to enhance such as maps as the CAVM to include information on the distribution of lichens.

It is worth remarking on the relationship between the approach adopted in the present paper, and the 'scaling ladder' approach (Wu 1999) discussed in the introduction. The coarse scale of the land-cover maps that we have investigated necessarily leads to a rather high degree of generalisation and few land-cover classes. The higher spatial resolution available from Landsat ETM+ imagery permits the reliable identification of a higher number (estimated at around 25) of land-cover classes, including (for example) the ability to distinguish between lichen-rich and lichen-poor areas, and it would be valuable to investigate the relationship between spatial resolution, or scale, and the number of distinguishable and useful land-cover classes for this area. This is not, however, the aim of this work. Instead, we have sought to identify which of a number of coarse-scale maps is closest to the true distribution of land-cover types. For this purpose, the fact that our chosen measure of nominal association is independent of the number of map classes is advantageous since it reduces the dependence of the results on scale. The two approaches may thus be seen as to some extent complementary.

## Conclusions

No circumpolar vegetation map currently gives an entirely adequate representation of tundra vegetation, as it relates either to climate or to reindeer husbandry. The best representation of those investigated in this study is currently provided by the Circumpolar Arctic Vegetation Map (CAVM). This is despite its rather high degree of generalisation. However, even this map does not sufficiently capture the distinction between dry and moist heath, or the extent of shrub vegetation, within our study area in Russia. The other two circumpolar (in fact global) vegetation maps that we studied proved to be rather far from optimal for arctic vegetation. The fact that none of the circumpolar maps distinguishes between areas rich and poor in lichen is a significant problem, especially when considering reindeer habitat.

While *in situ* mapping, or mapping based on the analysis of high-resolution multispectral imagery trained using field data, gives the most detailed and least generalised information about the distribution of vegetation, this is not an approach that can realistically be applied to synoptic vegetation mapping of the entire circumarctic region. Instead, it is probable that such maps will be derived from coarse-resolution data from sensors such as MODIS. Preliminary indications are that such data have the potential to map both shrubs and lichens, both poorly represented in the CAVM at present.

## Acknowledgements

Funding for this project was provided mainly through the EC-supported BALANCE programme, contract number EVK2-2002-00169, with additional support from St John's College, Cambridge. Both sources are gratefully acknowledged. Yasavei (the native people's organistion for the NAO) and NORUT IT, Tromsø, provided hospitality and assistance. The following individuals made valuable contributions to the work described in this paper: Florian Stammler (Scott Polar Research Institute), Christian Bay (Botanical Museum, University of Copenhagen), Lena Illinova, Bernt Johansen and Stein-Rune Karlsen (NORUT IT), Anatolii Aleksandrovich Taleev, Aleksei Aristarkovich Taleev, and the people of Brigade 5 of the Vyucheiskiy kolkhoz. We also express our gratitude to two anonymous reviewers for suggestions that have materially improved this paper.

## References

ACIA (Arctic Climate Impact Assessment). 2004. *Impacts of a warming Arctic*. Cambridge: Cambridge University Press.

Betts, R.A. 2000. Offset of the potential carbon sink from boreal forestation by decreases in surface albedo. *Nature* 408: 187–190.

Brown, J. F., T.R. Loveland, J.W. Merchant, B.C. Reed, and D.O. Ohlen. 1993. Using multisource data in global land cover characterization: concepts, requirements and methods. *Photogrammetric Engineering and Remote Sensing* 59: 977–987.

Cihlar, J., R. Latifovic, and J. Beaubien. 2000. A comparison of clustering strategies for unsupervised classification. *Canadian Journal of Remote Sensing* 26: 446–454.

Cohen, J. 1960. A coefficient of agreement for nominal scales. *Educational and Psychological Measurement* 20: 37–40.

Cornelissen, J.H.C., T.V. Callaghan, J.M. Alatalo, A. Michelsen, E. Graglia, A.E. Hartley, D.S. Hik, S.E. Hobbie, M.C. Press, C.H. Robinson, G.H.R. Henry, G.R. Shaver, G.K. Phoenix, D. Gwynn, S. Jonasson, F.S. Chapin, U. Molau, C. Neill, J.A. Lee, J.M. Melillo, B. Sveinbjörnsson, and R. Aerts. 2001. Global change and arctic ecosystems: is lichen decline a function of increases in vascular plant biomass? *Journal of Ecology* 89: 984–994.

Cramér, H. 1999. *Mathematical methods of statistics*. Princeton: Princeton University Press.

Eidenshink, J.C., and J.L. Faundeen. 1994. The 1 km AVHRR global land data set-first stages in implementation. *International Journal of Remote Sensing* 15: 3443–3462.

European Commission. 2003. Global land cover 2000 database. URL: http://www-gem.jrc.it/glc2000 (Last access 6 February 2006).

Finn, J. T. 1993. Use of the average mutual information index in evaluating classification error and consistency. *International Journal of Geographical Information Systems* 7: 349–366.

Gower, J. C. 1966. Some distance properties of latent root and vector methods used in multivariate analysis. *Biometrika* 53: 325–338.

Harding, R., P. Kuhry, T. Christensen, M.T. Sykes, R. Dankers, and S. van de Linden. 2002. Climate feedbacks at the tundra-taiga interface. *Ambio* (Special Report 12): 47–55.

Hinzman, L. D., N.D. Bettez, W.R. Bolton, F.S. Chapin, M.B. Dyurgerov, C.L. Fastie, B. Griffith, R.D. Hollister, A. Hope, H.P. Huntington, A.M. Jensen, G.J. Jia, T. Jorgenson, D.L. Kane, D.R. Klein, G. Kofinas, A.H. Lynch, A.H. Lloyd, A.D. McGuire, F.E. Nelson, W.C. Oechel, T.E. Osterkamp, C.H. Racine, V.E. Romanovsky, R.S. Stone, D.A. Stow, M. Sturm, C.E. Tweedie, G.L. Vourlitis, M.D. Walker, D.A. Walker, P.J. Webber, J.M. Welker, K.S. Winker, and K. Yoshikawa. 2005. Evidence and implications of recent climate change in northern Alaska and other arctic regions. *Climatic Change* 72: 251–298.

Hope, A., W. Boynton, D. Stow, and D. Douglas. 2003. Interannual growth dynamics of vegetation in the Kuparuk river watershed based on the normalized difference vegetation index. *International Journal of Remote Sensing* 24: 3413–3425.

Isachenko, T.I., E.M. Lavrinenko, S.A. Gribova, A.S. Karpenko, V.V. Lipatova, T.K. Yurkovskaya, A.A. Gerbikh, and G.D. Katenina. 1974. *Map of vegetation of the European part of the USSR*. Moscow: Chief administration of geodesy and cartography, Council of Ministers of the USSR.

Käyhkö, J., and P. Pellikka. 1994. Remote sensing of the impact of reindeer grazing on vegetation in northern Fennoscandia. *Polar Research* 13: 115–124.

Kershaw, K.A. 1985. *Physiological ecology of lichens*. Cambridge: Cambridge University Press.

Klein, D.R. 1999. The roles of climate and insularity in establishment and persistence of *Rangifer tarandus* populations in the high Arctic. *Ecological Bulletins* 47: 96–104.

Kumpula, J., A. Colpaert, and M. Nieminen. 2000. Condition, potential recovery rate, and productivity of lichen (*Cladonia* spp.) ranges in the Finnish reindeer management area. *Arctic* 53: 152–160.

Lunetta, R., and J.G. Lyon (editors). 2004. *Remote sensing and GIS accuracy assessment*. Boca Raton, Florida: CRC Press.

Marceau, D.J. 1999. The scale issue in social and natural sciences. *Canadian Journal of Remote Sensing* 25: 347–356.

Marceau, D.J., and G.J. Hay. 1999. Remote sensing contributions to the scale issue. *Canadian Journal of Remote Sensing* 25: 357–366.

Monserud, R.A., and R. Leemans. 1992. Comparing global vegetation maps with the Kappa statistic. *Ecological Modelling* 62: 275–293.

Myers, W., G.P. Patil, and C. Taillie. 1999. Cluster coordinated composites of diverse datasets on several spatial scales for designing extensive environmental sample surveys: prospectus on promising protocols.

In: Ghosh, S. (editor). *Multivariate analysis, design of experiments and survey sampling*. New York: Marcel Dekker Inc: 119–133.

Nordberg, M.-L., and A. Allard. 2002. A remote sensing methodology for monitoring lichen cover. *Canadian Journal of Remote Sensing* 28: 262–274.

Olson, J.S. 1994a. *Global ecosystem framework-definitions*. Sioux Falls, S.D: USGS Eros Data Center.

Olson, J.S. 1994b. *Global ecosystem framework-translation strategy*. Sioux Falls: USGS EROS Data Center.

Quattrochi, D.A., and M.F. Goodchild. 1997. *Scale in remote sensing and GIS*. Boca Raton, Florida: CRC Lewis.

Rees, G., I. Brown, K. Mikkola, T. Virtanen, and B. Werkman. 2002. How can the dynamics of the tundra-taiga boundary be remotely monitored? *Ambio* (Special Report 12): 56–62.

Rees, W. G., and O. Rigina. 2003. Methodologies for remote sensing of the environmental impacts of industrial activity in the Arctic and Sub-Arctic. In: Rasmussen, R.O., and N.E. Koroleva (editors). *Social and environmental impacts in the North*. Dordrecht: Kluwer: 67–88.

Rees, W. G., M. Williams, and P. Vitebsky. 2003. Mapping land cover changes in a reindeer herding area of the Russian Arctic using Landsat TM and ETM+ imagery and indigenous knowledge. *Remote Sensing of Environment* 85: 441–452.

Rees, W. G., O.V. Tutubalina, and E.I. Golubeva. 2004. Reflectance spectra of subarctic lichens between 400 and 2400 nm. *Remote Sensing of Environment* 90: 281–292.

Sandström, P., T. Granqvist Pahlén, L. Edenius, H. Tømmervik, O. Hagner, L. Hemberg, H. Olsson, K. Baer, T. Stenlund, L. Göran Brandt, and M. Egberth. 2003. Conflict resolution by participatory management: remote sensing and GIS as tools for communicating land-use needs for reindeer herding in northern Sweden. *Ambio* 32: 557–567.

Silapaswan, C., D. Verbyla, and D. McGuire. 2001. Land cover changes on the Seward Peninsula: the use of remote sensing to evaluate potential influences of climate change on historical vegetation dynamics. *Canadian Journal of Remote Sensing* 5: 542–554.

Skre, O., R. Baxter, R.M.M. Crawford, T.V. Callaghan, and A. Fedorkov. 2002. How will the tundra-taiga interface respond to climate change? *Ambio* (Special Report 12): 37–46.

Stow, D. A., A. Hope, D. McGuire, D. Verbyla, J. Gamon, F. Huemmrich, S. Houston, C. Racine, M. Sturm, K. Tape, L. Hinzman, K. Yoshikawa, C. Tweedie, B. Noyle, C. Silapaswan, D. Douglas, B. Griffith, G. Jia, H. Epstein, D. Walker, S. Daeschner, A. Petersen, L. Zhou, and R. Myneni. 2004. Remote sensing of vegetation and land-cover change in Arctic tundra ecosystems. *Remote Sensing of Environment* 89: 281–308.

Sturm, M., C. Racine, and K. Tape. 2001. Climate change: increasing shrub abundance in the Arctic. *Nature* 411: 546–547.

Théau, J. and C.R. Duguay. 2004. Lichen mapping in the summer range of the George River caribou herd using Landsat TM imagery. *Canadian Journal of Remote Sensing* 30: 867–881.

Théau, J., D.R. Peddle, and C.R. Duguay. 2005. Mapping lichen in a caribou habitat of northern Quebec, Canada, using an enhancement-classification method and spectral mixture analysis. *Remote Sensing of Environment* 94: 232–243.

Theil, H. 1972. *Statistical decomposition analysis*. Amsterdam: North Holland.

Tømmervik, H., K.A. Høgda, and I. Solheim, 2003. Monitoring vegetation changes in Pasvik (Norway) and Pechenga in Kola Peninsula (Russia) using multitemporal Landsat MSS/TM data. *Remote Sensing of Environment* 85: 370–388.

Tømmervik, H., B. Johansen, I. Tombre, D. Thannheiser, K.A. Høgda, E. Gaare, and F.E. Wielgolaski. 2004. Vegetation changes in the Nordic mountain birch forest: the influence of grazing and climate change. *Arctic, Antarctic and Alpine Research* 36: 323–332.

van de Linden, S., T. Virtanen, N. Oberman, and P. Kuhry. 2003. Sensitivity analysis of the discharge in the Arctic Usa basin, east-European Russia. *Climatic Change* 57: 139–161.

van Herk, C.M., A. Aptroot, and H.F. Dobben. 2002. Long-term monitoring in the Netherlands suggests that lichens respond to global warming. *Lichenologist* 3: 141–154.

Walker, D. A., C. Bay, F.J.A. Daniels, E. Einarsson, A. Elvebakk, B.E. Kapitsa, S.S. Kholod, D.F. Murray, S.S. Talbot, B.A. Yurtsev, and S.C. Zoltai. 1995. Toward a new Arctic vegetation map: a review of existing maps. *Journal of Vegetation Science* 6: 427–436.

Walker, D. A., W.A. Gould, H.A. Maier, and M.K. Raynolds. 2002. The circumpolar Arctic vegetation map: AVHRR-derived base maps, environmental controls, and integrated mapping procedures. *International Journal of Remote Sensing* 23: 4551–4570.

Wu, J. 1999. Hierarchy and scaling: extrapolating information along a scaling ladder. *Canadian Journal of Remote Sensing* 25: 367–380.